Interior Noise Considerations for Advanced High-Speed Turboprop Aircraft

J. S. Mixson,* F. Farassat,* and J. D. Leatherwood†
NASA Langley Research Center, Hampton, Virginia
and
R. Prydz‡ and J. D. Revell§
Lockheed California Company, Burbank, California

This paper describes recent research on noise generated by high-speed propellers, on noise transmission through acoustically treated aircraft sidewalls, and on subjective response to simulated turboprop noise. Propeller noise discussion focuses on theoretical prediction methods for complex blade shapes designed for low noise at Mach = 0.8 flight and on comparisons with experimental test results. Noise transmission experiments using a 168-cm-diam aircraft fuselage model and scaled heavy-double-wall treatments indicate that the treatments perform well and that the predictions are usually conservative. Studies of subjective comfort response in an anechoic environment are described for noise signatures having combinations of broadband and propeller-type tone components.

Introduction

HIGH-SPEED turboprop aircraft are being considered for development as passenger transports because of their fuel saving potential. However, new propellers and advanced noise control treatments are required to insure that the noise levels are acceptable to both passengers and community. Noise research on high-speed turboprops has been underway since 1976, and it is the purpose of this paper to report on the status of that work. Propeller source noise generation, noise transmission through the fuselage walls to the passenger cabin, and subjective comfort response in the passenger environment are considered. Structureborne noise, although a possible contributor to the passenger cabin noise level, is not considered since research results are not yet available for high-speed turboprops. Such noise may be generated by propeller or engine vibration, or by propeller wake impingement on wing or tail surfaces, and may transmit through the wing or fuselage structure.

Progress in interior noise research for high-speed turboprop aircraft has been summarized previously.[1,2] In this paper, attention will be focused on more recent results.

Noise of High-Speed Propellers

The development of quiet propellers for high-speed turboprop aircraft has included improved theoretical predictions[3,4] and tests of model propellers in a low-speed anechoic wind tunnel,[5,6] in a Mach = 0.8 hardwall tunnel (Ref. 7 contains a list of related papers including data), and in flight.[8] The lack of previous experience with the unique blade shapes used for high-speed flight, together with the desire to design for low noise, has placed unusual emphasis on theoretical prediction methods and on experimental verification of the theory. Previous theoretical methods are not suitable for the new blades and operating conditions; therefore extensive new developments have been required. In this paper, two theories are reviewed and predictions compared with results of tests in the anechoic wind tunnel. Comparisons with flight test results are currently being studied, but are not yet complete.

Theoretical noise prediction formulations have recently been reviewed and compared.[3] Two time domain formulations and one frequency domain formulation have been programmed for computers. Other formulations are possible, e.g., Ref. 9, but have not been programmed. The development of a computer program for prediction of advanced propeller noise is time consuming and costly due to the complex nature of the problem.

The Governing Equation

The governing differential equation for generation of noise by moving bodies[10-12] is known as the Ffowcs Williams-Hawkings equation (FW-H equation). Let the body in motion be described by $f(x,t) = 0$ in a frame fixed to the undisturbed medium in such a way that $f > 0$ outside the body. The FW-H equation is

$$\frac{1}{c^2}\frac{\partial^2 p'}{\partial t^2} - \nabla^2 p' = \frac{\partial}{\partial t}\left[\rho_0 v_n \left|\nabla f\right| \delta(f)\right] - \frac{\partial}{\partial x_i}\left[l_i \left|\nabla f\right| \delta(f)\right] + \frac{\partial^2}{\partial x_i \partial x_j}\left[T_{ij} H(f)\right] \quad (1)$$

where p' is the acoustic pressure, and ρ_0 and c are the density and speed of sound in the undisturbed medium, respectively. The local normal velocity of the body surface is $v_n = -(\partial f/\partial t)/|\nabla f|$ and l_i is the local force per unit area acting on the fluid at the surface of the body. The Lighthill stress tensor is denoted as T_{ij}. In the above equation, $\delta(f)$ and $H(f)$ are the Dirac delta function and the Heaviside function, respectively. The source terms on the right of Eq. (1) are known as the thickness, loading, and quadrupole sources, respectively. Nonlinear effects are taken into consideration through the quadrupole sources [the last term on the right side of Eq. (1)]. In the following solutions of the FW-H equation the quadrupole sources are not included.

The Farassat Method

This method depends on two solutions of the FW-H equation.[12] A computer program[13] and users manual[14] based on this method have been developed. The two solutions are as

Received June 16, 1982; presented as Paper 82-1121 at the AIAA/SAE/ASME 18th Joint Propulsion Conference, Cleveland, Ohio, June 21-23, 1982; revision received Nov. 1, 1982. This paper is declared a work of the U.S. Government and therefore is in the public domain.

*Aerospace Technologist. Member AIAA.
†Aerospace Technologist.
‡Research and Development Scientist.
§Research and Development Scientist. Associate Fellow AIAA.

follows:

$$4\pi p'(x,t) = \frac{1}{c}\frac{\partial}{\partial t}\int_{f=0}\left[\frac{\rho_0 c v_n + l_r}{r(1-M_r)}\right]_{\text{ret}} dS + \int_{f=0}\left[\frac{l_r}{r^2(1-M_r)}\right]_{\text{ret}} dS \tag{2}$$

$$4\pi p'(x,t) = \frac{\partial}{\partial t}\int_{\substack{f=0\\ g=0}}\frac{\rho_0 c v_n + l_r}{r\sin\theta}\, d\Gamma d\tau + \int_{\substack{f=0\\ g=0}}\frac{c l_r}{r^2\sin\theta}\, d\Gamma d\tau \tag{3}$$

In these equations, $r = |x-y|$; x is the observer position; y is the source position; and $M_r = v_i \hat{r}_i / c$ is the Mach number of the source in the radiation direction. Here $\hat{r}_i = (x_i - y_i)/r$ and $g = \tau - t + r/c$, where τ and t are the source and observer times, respectively. The curve Γ in Eq. (3) is the intersection of the body $f=0$ with the event sphere (collapsing sphere) $g=0$. The angle θ is between the normal to the body and the radiation direction $\hat{r}_i$. The subscript ret refers to retarded time.

Equations (2) and (3) are used as follows.[13,14] The blade surface is divided into panels. If the panel center has a single emission time and M_r at emission time is less than a prescribed value (very near 1), Eq. (2) is used to calculate the contribution of the panel to the acoustic pressure. Otherwise Eq. (3) is used. The observer in these acoustic calculations may be stationary with respect to the medium or in motion with the aircraft. There is no analytic approximation necessary for the case of a moving observer.

Figure 1 shows an acoustic signature for the advanced blade shape (designated SR-3) shown in Fig. 2. The propeller is designed for eight blades and Mach = 0.8 flight but was tested with four blades due to test hardware limitations, and with overspeed rpm to get the design tip speed with the low tunnel speed (Table 1). The microphone position in the theoretical calculations[13] was corrected for the tunnel jet shear layer. The agreement between theory and experiment shown in Fig. 1, along with results for other blade shapes and microphone positions[13] indicates that the acoustic pressures can be predicted within a few decibels. The high-frequency differences come from numerical errors which can be corrected by using a large number of panels on the blade (time consuming on a computer) or using numerical filtering. Other possible sources of error are the theoretical approximation of the blade chordwise and spanwise aerodynamic loading, tunnel shear layer correction, and the neglect of nonlinear effects. New formulations of the equations have been made[15] to reduce computation time and to improve accuracy.

Hanson's Methods

Hanson has developed two methods, one in the time domain and one in the frequency domain.[4,16]

In the time domain the acoustic planform (APF) is defined as the intersection of the collapsing sphere $g = \tau - t + r/c = 0$ and the blade mean surface. Then the acoustic pressure $p'(x,t)$ is calculated from

$$4\pi p'(x,t) = \frac{1}{c}\frac{\partial}{\partial t}\int_{\text{APF}}\frac{1}{r}\left[2\rho_0 c v_n - \Delta p\cos\theta\right]_{\text{ret}} d\Sigma - \int_{\text{APF}}\frac{1}{r^2}\left[\Delta p\cos\theta\right]_{\text{ret}} d\Sigma \tag{4}$$

where $d\Sigma$ is the element of area of the acoustic planform. Also $\Delta p = p_{\text{lower}} - p_{\text{upper}}$, where p_{lower} and p_{upper} stand for the surface pressure on the lower and the upper surfaces of the blade, respectively. Note that v_n on one side of the blade must be used. In the application of Eq. (4), the time derivative is taken numerically. This equation can be shown to be related to Eqs. (2) and (3). Approximations involved in Eq. (4) are discussed in Ref. 3.

The frequency domain formulation describes the amplitude in the far field of the harmonics of the propeller noise.[16] It is somewhat more complicated than Eqs. (2-4), but is equivalent to the Fourier transform of the equations.

The details of Hanson's computer programs have not been published. Unpublished numerical results obtained by Hanson and Farassat have been found to agree very closely for an advanced propeller when identical input values are used.

Other Considerations

The above equations depend on the normal velocity and the aerodynamic force distributions on the blade surface. The predicted noise levels are quite sensitive to the velocities and forces; therefore, to insure accuracy, detailed accurate input

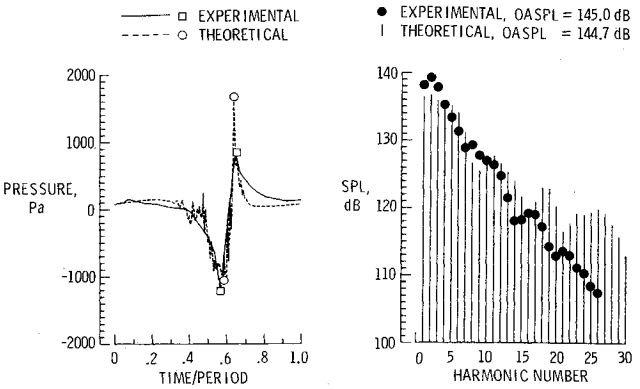

Fig. 1 Acoustic signature and spectrum of an advanced propeller. Microphone is 0.04 m forward of propeller plane and 0.808 m from propeller axis.

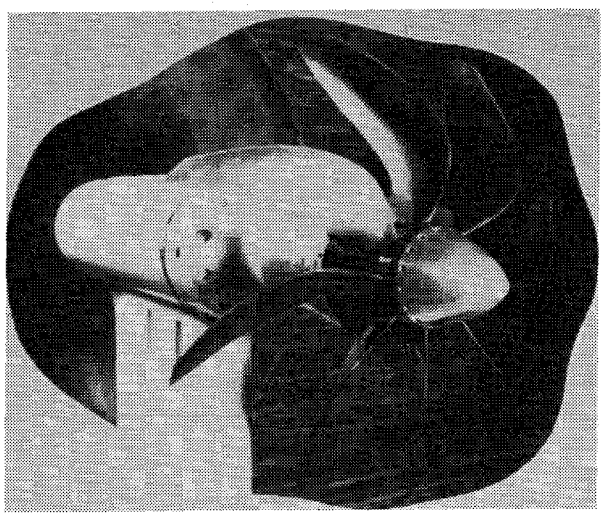

Fig. 2 Model of an advanced propeller in an anechoic wind tunnel; 65 cm diameter.

Table 1 Operating conditions and blade data for anechoic wind tunnel tests[5]

Blade radius, m	0.324
Number of blades	4
Rotational speed, rpm	11,250
Tunnel Mach number	0.32
Helical tip Mach number	1.17
Ambient temperature, °C	13.3
Ambient pressure, kPa	94.6
Blade angle at $(\eta_2/R)_{\text{ref}} = 0.776$, deg	25.2

data must be used. In recent calculations for general aviation propellers,[2] surface pressures were calculated using two-dimensional aerofoil codes for use in the theory and good agreement with measured noise was obtained. However, in general, the precise surface pressure needed for input to the acoustic program has not been available. In addition, some tunnel test conditions (shear layer, hardwalls) have increased the difficulty of validating the theory, which applies to an infinite stationary acoustic medium.

Hanson and Fink have considered the inclusion of quadrupole sources connected with the blade system.[17] They found that in the transonic range, the noise due to quadrupoles has a directivity similar to the thickness noise. It can also have levels of the order of magnitude of thickness noise, particularly for thick blades. However, it appears[17] that for advanced turboprop blades with thin sections and large sweep, nonlinear effects are minimal.

Fuselage Noise Transmission

Theoretical Studies

Noise transmission into the passenger cabin of aircraft powered by advanced propellers has been studied as part of systems evaluations of the potential fuel savings of turboprops in comparison with turbofan propulsion.[18-20] These studies have shown worthwhile fuel savings using turboprops and have estimated the weight required for fuselage sound insulation. More extensive theoretical studies have been done to develop improved methods for analysis and design of sound insulation, to refine the weight estimates, to define specific configurations of sidewall insulation, and to explore ways to obtain lighter weight insulation.[21-24] These studies confirmed the weight estimates made in the earlier systems studies. Sidewall insulation configurations are presented for a variety of aircraft sizes and construction types. In particular, it is shown that a satisfactory cabin environment can be obtained using insulation materials and configurations in current operational usage. However, the noise reduction and weight of these configurations are higher than any existing aircraft insulation systems, indicating a need for experimental tests to verify the performance of the insulation, to verify the theoretical methods, and to gain experience with the new heavy insulation. The tests described below were carried out at the Lockheed-California Company.

Fuselage Test Model

In order to obtain maximum data in a controlled test environment within cost constraints, a reduced-scale fuselage model was used (Fig. 3). The full-scale aircraft of interest are narrow body conventional configurations. In order to have specific numbers to work with, fuselage wall design No. 8 of Ref. 21 was chosen as an example.

The model is a section of fuselage taken from an operational commuter-class aircraft in order to save cost and to obtain realistic construction (Fig. 4). The test section was chosen in an area where the fuselage has constant diameter and skin thickness and uniform spacing of rings and stringers. The remainder of the fuselage length was retained in order to provide realistic interior acoustic characteristics. For these tests, regions of the fuselage other than the test section were treated with heavy insulation to prevent flanking acoustic transmission to the interior. Therefore the test could yield clear indications of the performance of the treatment applied in the test section. Open-pore acoustical foam was placed in the interior to simulate the absorption characteristics of an aircraft cabin. This configuration is felt to be reasonable because propeller noise is heavily concentrated near the plane of rotation.

The floor (Fig. 5) is located at a scaled height appropriate for a CTOL aircraft and is supported only on air springs (no contact at the floor-sidewall juncture) to prevent flanking acoustic transmission. The trim panel consists of a single sheet of aluminum in the circumferential direction and is supported only at the floor by an isolator. The interior noise levels are measured at a scaled height representing ear level for a seated passenger, and at several radial locations. The acoustic treatment consists of layers of mass-loaded vinyl glued to the skin or trim panel and fiberglass blankets in the wall cavity. Vinyl of 4.9 kg/m^2 was used in one or two layers to obtain mass values covering a range that includes the values scaled from Ref. 21 (Table 2). The trim panel spacing from the skin (Fig. 5b) was also scaled from design 8 of Ref. 21.

The diameter is chosen as the primary scaling length, giving a scale factor of 0.43. The assumption that all model dimensions reduce by the scale factor results in the scaled

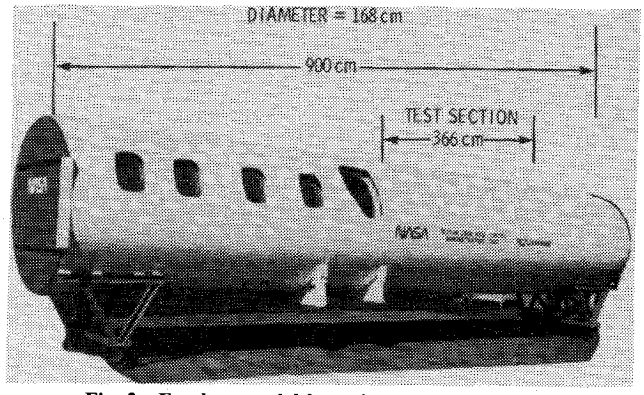

Fig. 3 Fuselage model for noise transmission tests.

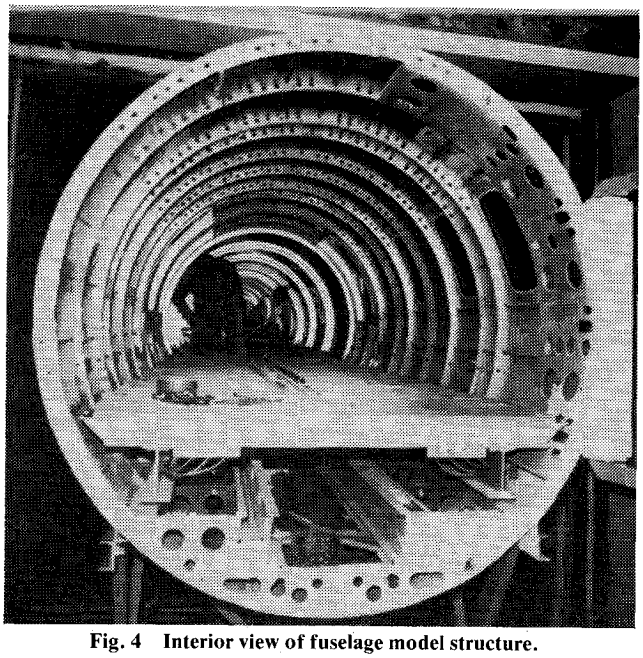

Fig. 4 Interior view of fuselage model structure.

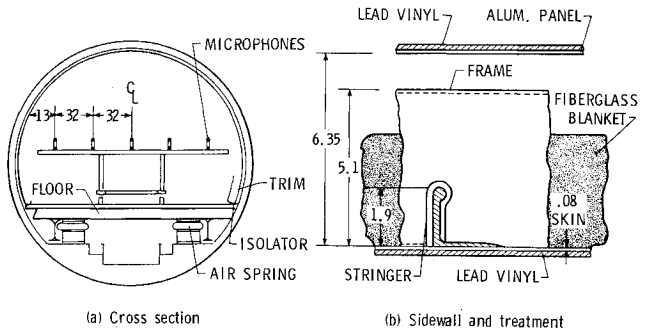

Fig. 5 Fuselage model structure and dimensions (in centimeters); 168 cm diameter.

Table 2 Comparison of fuselage model with scaled properties: scale factor = 0.43

	Full scale[21]	Scaled	Test model
Diameter, cm	391	168	168
Skin thickness, cm	0.114	0.05	0.10
Frame:			
Depth, cm	15.2	6.5	5.1
Spacing, cm	48.3	20.7	38.1
Area, cm^2	2.5	0.46	0.88
Stringer:			
Depth, cm	3.1	1.3	1.9
Spacing, cm	15.2	6.5	17.8
Area, cm^2	0.94	0.17	0.72
Outer wall weight, M_0, kg/m^2	19.6	8.4	4.6 9.5
Trim panel weight, M_T, kg/m^2	13.4	5.8	2.2 7.1 12.0

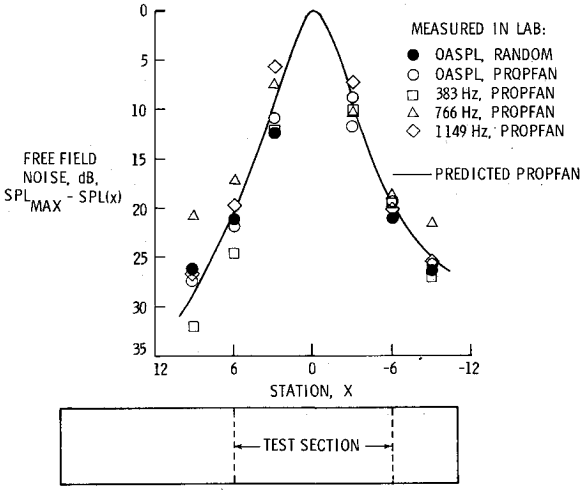

Fig. 6 Source noise distribution for fuselage model tests.

values in Table 2. The table shows that the depth of the frames and stringers are approximately to scale, but the spacings are larger than scaled values. However, the areas of frame and stringer and the skin thickness are larger than scaled values, which should provide some increased stiffness in compensation for the reduced stiffness associated with the large spacing. Flat panel tests suggest that the differences in stiffener configuration result in only small transmission effects at the propfan frequencies. Theoretical studies[24] indicated that in-plane loads due to pressurization need not be simulated in the model.

Test Conditions

The tests were carried out with the fuselage model in an anechoic chamber. An acoustic horn was used to generate the test noise signals and was located at the midpoint of the test section. The noise distribution is shown in Fig. 6. The distributions are normalized so all values are 0 dB at station 0. The lab distribution is seen to be in close agreement with the prediction and is about 20 dB down from the peak value at locations outside the test section. The spectrum in narrow bands is reasonably flat from about 300 to about 1300 Hz. The results presented here were obtained using the broadband spectrum with peak SPL values of approximately 130 dB.

Interior Noise Distributions

Interior noise pressures were recorded using the radial microphone array shown in Fig. 5, located at 15 longitudinal stations from −10.5 to +10.5 for each sidewall configuration. The stations indicate the longitudinal distance in

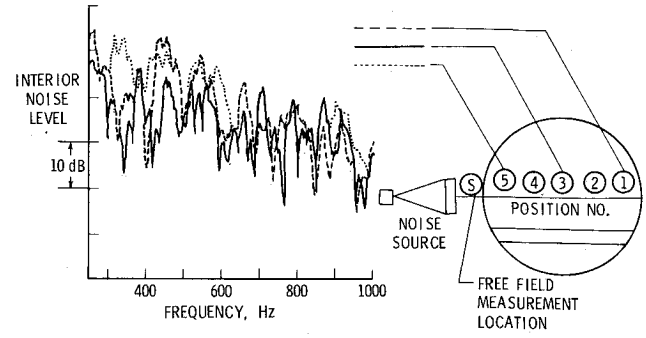

Fig. 7 Variation of interior noise across model width. On source axis (station 0). Outer wall = 4.6 kg/m^2, trim panel = 7.1 kg/m^2.

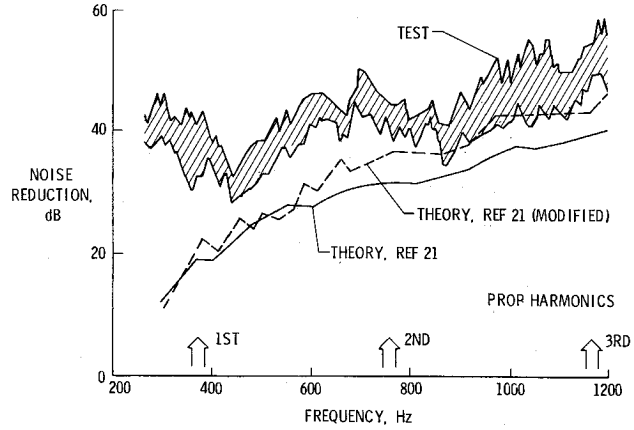

Fig. 8 Fuselage noise reduction for lighter sidewall, $M_0 = 4.6$ kg/m^2, $M_T = 2.2$ kg/m^2.

feet from the midpoint of the test section (Fig. 6). The distribution of overall noise level did not vary much over the test section but dropped off at positions outside the test section due to the absorption inside the model. Figure 7 shows narrow-band spectra of interior noise for the three radial positions indicated at the right of the figure. (The spectra for positions 2 and 4 lie generally within the envelope of the spectra shown.) Figure 7 shows no systematic variation of noise over the width of the model. At some frequencies, position 5 is higher than the other two, e.g., 350 and 600 Hz, while at other frequencies position 1 is the highest, e.g., peaks at about 450 and 650 Hz. There are many frequencies where the levels are close together for all three positions.

Noise Reduction

Noise reduction is defined as the difference between the noise level in the anechoic chamber without the fuselage present (measured at the intersection of the fuselage sidewall position and the noise source axis) and the noise level inside the fuselage model. This definition is used to conform to the theoretical definition.[21] Pressures on the sidewall are expected to be no more than 6 dB higher[6] than the free field values used in this definition. For both measurements the noise source characteristics are held constant and all other features of the test chamber are unchanged. When the fuselage is not present, the reference noise level is measured at station 0, i.e., at the peak of the longitudinal noise distribution (Fig. 6), at a distance from the horn corresponding to the position the fuselage occupies when present in the chamber. This position is indicated by the S in Fig. 7. The noise reduction data in Figs. 8 and 9 are the envelope of the spectra obtained by averaging radially for each of the stations −3, −1.5, 0, 1.5, and 3 and by averaging longitudinally over these stations for microphones 1 and 5.

Figures 8 and 9 indicate that the agreement between measured and predicted values of noise reduction depends

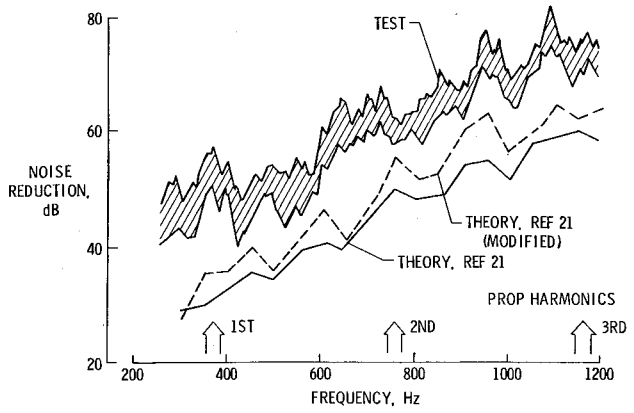

Fig. 9 Fuselage noise reduction for heavier sidewall, $M_0 = 9.5$ kg/m^2, $M_T = 7.1$ kg/m^2.

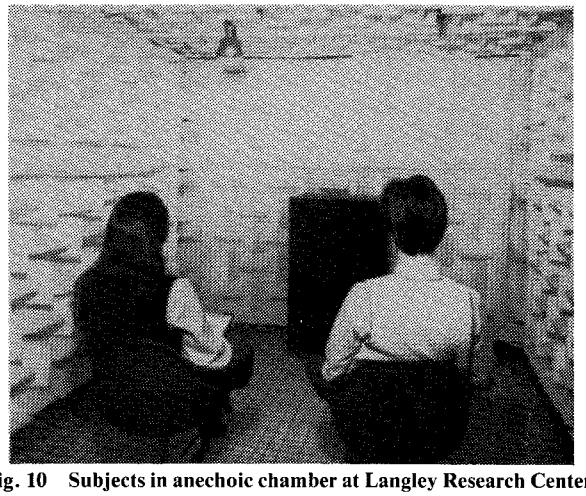

Fig. 10 Subjects in anechoic chamber at Langley Research Center.

somewhat on sidewall mass. The propeller harmonics indicate the scaled values of the harmonics for the full-scale propfan design. The interior noise A-weighted level was found to be governed by the first three harmonics,[21,24] indicating that these figures cover the frequency range that is important for interior noise prediction. The theory of Ref. 21 lies below the data. The exterior noise in the theory is constant over the test section, but varies in the test (Fig. 6). The correction to account for this is estimated as a reduction of the test noise reduction values by about 7 dB. The (scaled) sidewall mass of Fig. 9 is the value required to provide the high noise reduction needed for a comfortable interior noise level.[21] Therefore the sidewalls are performing in the tests somewhat better than predicted, and the results of Ref. 21 can be considered to be conservative (for the propeller noise levels and interior noise criteria used in that reference).

For the lighter weight sidewall (Fig. 8), the theory of Ref. 21 tends to fall somewhat closer to the data except at frequencies below 400 Hz. This result, together with the underprediction in Fig. 9, indicates that improvements in the theory are desirable. The analysis of Ref. 25 indicated that improved agreement with data was obtained when an acoustic loss factor was included in addition to the propagation constant previously used[21] for the airspace between the outer wall and the trim panel. The dashed line indicates predictions made using the theory of Ref. 21 as modified with the loss factor and an improved representation of the cabin acoustics. The figures show that this analysis usually predicts higher noise reductions than the previous theory. However, further basic theoretical development appears to be required.

Passenger Response

Previous Work

The previous sections of this paper described propeller source noise and transmission of this noise into the passenger cabin. It was indicated that the turboprop interior noise environment consists of high-level low-frequency tones, in contrast to the broadband higher frequency noise of current turbofan aircraft. It is particularly important to understand the response of passengers to the tonal propeller noise so the increased fuel efficiency of advanced turboprops will not be compromised by negative passenger reaction or increased sidewall weight for noise control. Previous studies[2,26,27] have indicated that pure tones combined with bands of noise were generally rated noisier or more annoying than the bands of noise alone for equal overall sound pressure levels. This would imply that tones in the passenger cabin of a turboprop aircraft could result in increased passenger annoyance unless the levels are reduced. Progress on the determination of the degree and extent of the increased annoyance is the subject of this section.

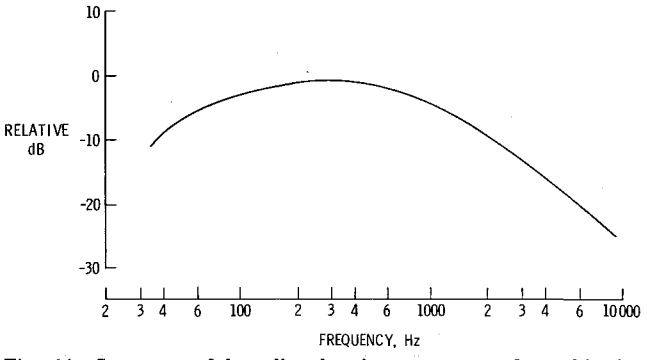

Fig. 11 Spectrum of broadband noise component for subjective tests.

Anechoic Environment Tests

The objectives of these studies include determination of the effects of the frequency and amplitude of tones added to simulated boundary-layer noise and examination of various metrics for quantifying passenger response to the combined tone and noise environment. Results of two recent studies are described. The first study was designed to obtain baseline annoyance responses to boundary-layer noise alone, and the second obtained annoyance responses to single tones combined with boundary-layer noise. Both studies were conducted in the anechoic listening room shown in Fig. 10. In this room two subjects can be exposed to selected noises in a nonreverberant environment.

Noise Stimuli

Two acoustical components were used to simulate the interior noise environment of a turboprop aircraft. These were 1) broadband noise due to the turbulent boundary layer on the aircraft fuselage, and 2) a tone due to the fundamental blade passage frequency of the propeller. The boundary-layer spectrum shape is illustrated in Fig. 11. This curve was generated using estimates of external boundary-layer noise and sidewall noise transmission. At frequencies above 1000 Hz the curve is somewhat higher than measured interior spectra, with the difference depending on the aircraft size and position in the cabin. One-third octave band spectra were generated in the shape shown in Fig. 11 by spectrally shaping the output of a pink noise signal source. The tones were generated by a signal oscillator and were mixed with the boundary-layer noise by means of an electronic summing network. In the study to determine baseline annoyance responses the stimuli consisted of only boundary-layer noise applied at A-weighted levels ranging from 63 to 90 dB. The second study mixed single tones with the boundary-layer

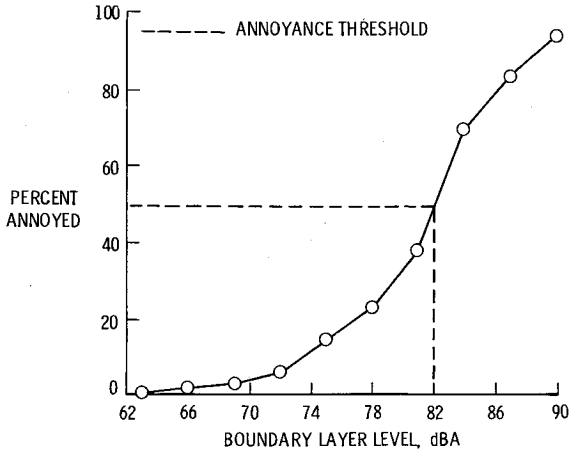

Fig. 12 Cumulative distribution of subjective response to broadband noise.

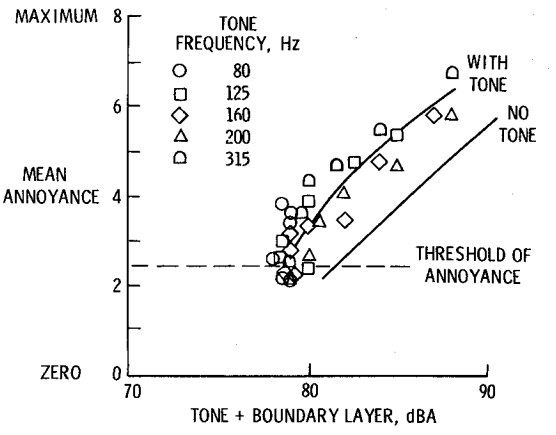

Fig. 13 Subjective response to combined noise signatures. Broadband level for tone tests = 78 dBA.

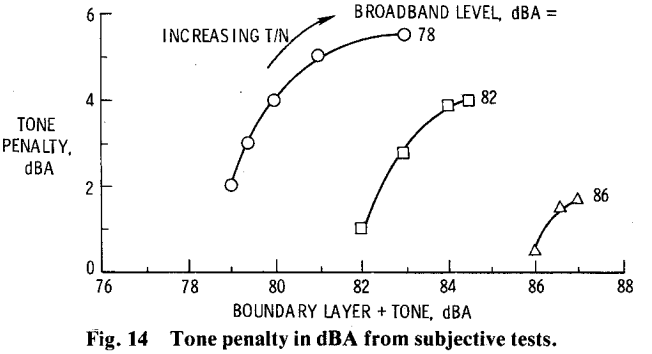

Fig. 14 Tone penalty in dBA from subjective tests.

noise. Boundary-layer A-weighted noise levels of 78, 82, and 86 dB were combined with single tones having frequencies of 80, 125, 160, 200, and 315 Hz. Tone/noise ratios depended upon tone frequency and ranged from −3 to 33 dB. Tone/noise ratio is defined as the difference (in decibels) between the sound pressure level of the tone at the propeller blade passage frequency and the boundary-layer noise level in the one-third octave band containing the tone frequency.

Test Design

In the first study the subjects were asked to rate various boundary-layer noise stimuli as either annoying or not annoying. The stimuli had identical spectral characteristics and differed only in terms of A-weighted sound pressure level. A total of 28 subjects experienced each of the boundary-layer noise levels which were randomized and counterbalanced before presentation.

In the second study, 120 noise stimuli were formed from factorial combinations of five tone frequencies (80, 125, 160, 200, 315 Hz), three boundary-layer levels (78, 82, 86 dBA), and eight tone levels (70-98 dB). Subjective responses were obtained using both a dichotomous (annoying/not annoying) scale and a unipolar eight-point category scale anchored by the adjectives "not annoying" and "extremely annoying." Both studies used signal durations of about 30 s.

Results

Annoyance threshold for the boundary-layer noise is defined as the A-weighted level at which 50% of the subjects were annoyed. This level was determined from the data of Fig. 12, which give the proportion of subjects, at each boundary-layer level, that rated that level as annoying. The dashed lines indicate that annoyance threshold was approximately 82 dBA. This reflects the annoyance threshold in the absence of tones and provided the basis for selecting the noise levels used in the second study.

The effect of adding single tones at each frequency to a boundary-layer noise level of 78 dBA is shown in Fig. 13. This figure indicates that the mean annoyance ratings (averaged over subjects) increased as the A-weighted sound pressure level of the combined stimuli increased. Since boundary-layer noise level was constant, the increase in combined level was due to the presence of the tone, i.e., increasing tone/noise ratio. Included for comparison is the annoyance response curve for boundary-layer noise alone with the threshold of annoyance indicated by the dashed line. These data show that, for equal A-weighted sound pressure levels, the combinations of tones and noise were evaluated as more annoying than the noise presented alone. Another way of interpreting the data of Fig. 13 is as follows: Adding a single tone to boundary-layer noise presented at 78 dBA results in a level of subjective annoyance equivalent to that produced by tone-free boundary-layer noise applied at a significantly higher level. This implies that the presence of tones in the boundary-layer noise acts to reduce passenger acceptance. The extent of the penalty can be defined in Fig. 13 as the difference, for a constant value of annoyance, between the A-weighted sound pressure level of the boundary-layer noise without tones and the corresponding A-weighted level with tones added. The penalties are summarized in Fig. 14 for all three boundary-layer noise levels investigated. Tone penalties for the 78-dBA boundary-layer noise ranged from approximately 2 dB at low tone/noise ratios to about 5 dB at the highest tone/noise ratios. (The lowest tone levels used were high enough to result in an increase to 79 dBA when the tone was added to the 78-dBA broadband level.) For the larger boundary-layer noise levels the tone penalties decreased, implying that the boundary-layer noise began to mask the tonal components. The amount of the penalty may also vary depending on the particular spectrum shape used for the broadband component.

Table 3 Correlation coefficients between subjective annoyance responses and OASPL, dBA, PNL, and PNLT

Boundary-layer level, dBA	OASPL	dBA	PNL	PNLT
78	0.888	0.891	0.906	0.841
82	0.900	0.856	0.898	0.888
86	0.672	0.735	0.648	0.841

The ability of several metrics (OASPL, dBA, PNL, PNLT) to quantify passenger annoyance to the interior noise environment used in these studies was examined by computing the correlation coefficients between annoyance responses and

each metric. These are summarized in Table 3 for each level of boundary-layer noise. The correlation coefficients within each noise level were based upon the annoyance responses for all frequencies. These data indicate that each metric generally performed well, particularly at the two lowest boundary-layer noise levels. Thus there is no justification, based upon these data, for selecting a "best" metric for quantifying the interior noise environment. However, since the penalties discussed earlier were determined in terms of A-weighted sound pressure level, and, since this metric is easily measured, it should be considered as a prime candidate for use in assessing turboprop interior noise.

Concluding Remarks

This paper describes recent research related to interior noise of aircraft powered by advanced high-speed turboprops. The theoretical methods of Farassat and Hanson for predicting the noise generated by propellers are reviewed. Comparisons of predictions with measurements from a 65-cm-diam model in an anechoic wind tunnel suggest good agreement. Sidewall noise transmission results are presented from tests of a 168-cm-diam aircraft fuselage model. The theory is shown to be conservative for the high values of mass, and differences from test results suggest that improved theory would be desirable. Subjective response to noise signatures containing broadband and tone components is described as measured in an anechoic laboratory facility. Results indicate that the signatures containing tones are rated as less desirable by the subjects.

References

[1]Dugan, J.F., Miller, B.A., Graber, E.J., and Sagerser, D.A., "The NASA High Speed Turboprop Program," NASA TM 81561, Oct. 1980.

[2]Mixson, J.S., Greene, G.C., and Dempsey, T.K., "Sources, Control and Effects of Noise from Aircraft Propellers and Rotors," NASA TM 81971, April 1981.

[3]Farassat, F., "Linear Acoustic Formulas for Calculation of Rotating Blade Noise," *AIAA Journal,* Vol. 19, Sept. 1981, pp. 1122-1130.

[4]Hanson, D.B., "Near Field Noise of High Tip Speed Propellers in Forward Flight," AIAA Paper 76-565, Sept. 1976.

[5]Brooks, B.M. and Metzger, F.B., "Acoustic Test and Analysis of Three Advanced Turboprop Models," NASA CR 159667, Jan. 1980.

[6]Magliozzi, B. and Brooks, B.M., "Advanced Turboprop Airplane Interior Noise Reduction-Source Definition," NASA CR 159668, Oct. 1979.

[7]Dittmar, J.H. and Rice, E.J., "A Shock Wave Approach to the Noise of Supersonic Propellers," NASA TM 82752, Dec. 1981.

[8]Mackall, K.G., Lasagna, P.L., and Dittmar, J.H., "In-Flight Acoustic Results from Two Advanced Design Propellers at Mach Numbers up to 0.8," AIAA Paper 82-1120, June 1982.

[9]Jou, W.-H., "Supersonic Propeller Noise in a Uniform Flow," AIAA Paper 79-0348, 1979.

[10]Ffowcs Williams, J.E. and Hawkings, D.L., "Sound Generated by Turbulence and Surfaces in Arbitrary Motion," *Philosophical Transactions of the Royal Society of London, Series A,* Vol. 264, 1969, pp. 321-342.

[11]Farassat, F., "Discontinuities in Aerodynamics and Aeroacoustics: The Concept and Application of Generalized Derivatives," *Journal of Sound and Vibration,* Vol. 55 Part (2), 1977, pp. 165-193.

[12]Farassat, F., "Theory of Noise Generation from Moving Bodies with an Application to Helicopter Rotors," NASA TR R-451, 1975.

[13]Nystrom, P.A. and Farassat, F., "A Numerical Technique for Calculation of the Noise of High Speed Propellers with Advanced Geometry," NASA TP 1662, 1980.

[14]Martin, R.M. and Farassat, F., "User's Manual for a Computer Program to Calculate Discrete Frequency Noise of Conventional and Advanced Propellers," NASA TM 83135, 1981.

[15]Farassat, F., "Advanced Theoretical Treatment of Propeller Noise," von Karman Institute Lecture Series 1982-08, *Propeller Performance and Noise,* Rhode Saint Genese, Belgium, May 24-28, 1982.

[16]Hanson, D.B., "The Influence of Propeller Design Parameters on Far-Field Harmonic Noise in Forward Flight," AIAA Paper 79-0609, 1979.

[17]Hanson, D.B. and Fink, M.R., "The Importance of Quadrupole Sources in Prediction of Transonic Tip Speed Propeller Noise," *Journal of Sound and Vibration,* Vol. 62 Part (1), 1979, pp. 19-38.

[18]"Energy Consumption Characteristics of Transports Using the Propfan Concept," NASA CR 137937, Nov. 1976.

[19]Revell, J.D. and Tulis, R.H., "Fuel Conservation Merits of Advanced Turboprop Transport Aircraft," NASA CR 152096, Aug. 1977.

[20]Goldsmith, I.M., "A Study to Define the Research and Technology Requirements for Advanced Turbo/Propfan Transport Aircraft," NASA CR 166138, Feb. 1981.

[21]Revell, J.D., Balena, F.J., and Koval, L.R., "Analytical Study of Interior Noise Control by Fuselage Design Techniques on High-Speed Propeller Driven Aircraft," NASA CR 159222, July 1978.

[22]Revell, J.D., Balena, F.J., and Koval, L.R., "Analysis of Interior Noise Control Treatments for High-Speed Propeller-Driven Aircraft," *Journal of Aircraft,* Vol. 19, Jan. 1982, pp. 31-38.

[23]Revell, J.D., Balena, F.J., and Koval, L.R., "Interior Noise Control by Fuselage Design for High-Speed Propeller-Driven Aircraft," *Journal of Aircraft,* Vol. 19, Jan. 1982, pp. 39-45.

[24]Rennison, D.C., Wilby, J.F., Marsh, A.H., and Wilby, E.G., "Interior Noise Control Prediction Study for High-Speed, Propeller-Driven Aircraft," NASA CR 159200, Sept. 1979.

[25]Balena, F. and Prydz, R., "Experimental and Predicted Noise Reduction of Stiffened and Unstiffened Cylinders With and Without a Limp Inner Wall," AIAA Paper 81-1968, Oct. 1981.

[26]Kryter, K.D. and Pearsons, K.S., "Some Effects of Spectral Content and Duration on Perceived Noise Level," *Journal of the Acoustical Society of America,* Vol. 35, June 1963, pp. 866-883.

[27]Kryter, K.D. and Pearsons, K.S., "Judged Noisiness of a Band of Random Noise Containing an Audible Pure Tone," *Journal of the Acoustical Society of America,* Vol. 38, April 1965, pp. 106-112.